Asian Journal of Chemistry Vol. 20, No. 5 (2008), 3438-3446

Synthesis of *cis*-Dithiocyanato *bis*(4,4'-Dicarboxylic acid-2,2'-bipyridine)ruthenium and its Application in Dye-Senstized Solar Cells

SONG WANG, XIAO HONG WU * and ZHAO HUA JIANG
Harbin Institute of Technology, Harbin, 150001, P.R. China
Fax: (86)(451)86402522; Tel: (86)(451)86402522
E-mail: wxhqw@263.net

cis-Dithiocyanato *bis*(4,4'-dicarboxylic acid-2,2'-bipyridine) ruthenium was synthesized from 4-methylpyridine by the reactions of cross-coupling, oxidation, conjugating reaction and ligand substitution reaction. The product and its intermediates were characterized with IR spectrum, GC-MS, NMR and elemental analysis. TiO_2 films were obtained by sol-gel method and these films were sensitized by *cis*-$RuL_2(SCN)_2$ (L = *cis*-2,2'-bipyridine-4,4'-dicarboxlic acid). UV and IR absorption spectroscopy of the sensitized film indicated that the *cis*-$RuL_2(SCN)_2$ has attached to the surface of the TiO_2 particles. In addition, *cis*-$RuL_2(SCN)_2 \cdot 2H_2O$ applications in dye-sensitized solar cells were demonstrated. From the I-V curves, the open-circuit voltage (V_{OC}) and short-circuit current (I_{SC}) were also measured.

Key Words: Ruthenium, 4-Methylpyridine, TiO_2 film.

INTRODUCTION

In recent years, there had been a growing interest in photoelectrochemical devices based on nanocrystalline TiO_2 sensitized with transition metal complexes[1]. Although the considerable progress made in the past decade towards improving of the photoelectricity properties, comparatively less work on the progress of synthesizing the sensitizers. Among of all kind of known sensitizers, the performance of the *cis*-$RuL_2(SCN)_2 \cdot 2H_2O$ was found to be outstanding. At present, most of the methods use 2,2'-bipyridine-4,4'-dimethyl as the initial material. But the cost of 2,2'-bipyridine-4,4'-dimethyl is relatively expensive. So in order to decline the cost, we synthesized 2,2'-bipyridine-4,4'-dimethyl from 4-methylpyridine and then synthesized *cis*-$RuL_2(SCN)_2 \cdot 2H_2O$.

2,2'-Bipyridine-4,4'-dimethyl is an important intermediate used to synthesize *cis*-$RuL_2(SCN)_2 \cdot 2H_2O$ in the area of nanocrystalline photovoltaic cells (NPC)[2,3]. 2,2'-Bipyridine-4,4'-dimethyl is a compound that belongs to 2,2'-bipyridine series, so the methods of synthesizing 2,2'-bipyridine-4,4'-

dimethyl is as the same as the methods used to synthesize 2,2'-bipyridine. In the recent years, researchers had tried to use catalysts such as nickel complexes and palladium complexes, which are widely used in the area of coupling reaction[4,5] hydrogenation reaction[6] and dehydrogenation reaction[7]. But these methods couldn't be used to synthesize 2,2'-bipyridine-4,4'-dimethyl directly, because the material they used was halopyridine. So we have to adopt another method to prepare 2-aryl-4-methylpyridine, which results in low yield, time-wasting and high cost. Herein according to our former work, we found the way of synthesizing *cis*-$RuL_2(SCN)_2$.

EXPERIMENTAL

Synthesis of *cis*-$RuL_2(SCN)_2$: *cis*-$RuL_2(SCN)_2$ was prepared in four steps using 4-methyl-bipyridine. ^1H NMR and ^{13}HMR were obtained on a Brucker AV 300, 300 MHz spectrometry, using TMS as an internal standard. IR spectra were performed on an Avatar 360 FT-IR Spectrometry and the elemental analyses were recorded using a Thermo Finnigan Eager 300. GC-MS spectrum was obtained on 5973N GC/MSD (Agilent Technologies, U.S.A).

Synthesis of 4,4'-dimethyl-2,2'-bipyridine: The 4-methylpyridine was redistilled in order to eliminate the pigments and other impurities. 25.0 g of 4-methylpyridine (268 mmol) and 0.5 g palladium-catalyst were mixed together and heated at reflux for 3 d. Then, the reaction mixture was filtered by suction filtration in order to filter off the palladium-catalyst. The recovery ratio of palladium-catalyst is 90 % and it can be used repeatedly. The filtrate was evaporated to dryness on a rotary evaporator, which can obtain 18.5 g of 4-methyl-pyridine and the pale-yellow solid (4,4'-dimethyl-2,2'-bipyridine). The filter cake was washed with hot acetic ester. The obtained 4,4'-dimethyl-2,2'-bipyridine was transferred into the hot washing liquid and then was recrystallized affording the 4.6 g (24.9 mmol) of product 4,4'-dimethyl-2,2'-bipyridine as a white solid. In this way, the purity is higher than 99 % and the yield is 70.8 %.

2,2'-Bipyridyl-4,4'-dicarboxylic acid: It was prepared according to a previously described procedure[8]. 4.6 g of 4,4'-dimethyl-2,2'-bipyridine was dissolved in 50 mL of conc. sulfuric acid with vigorous stirring using a magnetic stirrer. After the solution was cooled at 0 ºC and 15 g of CrO_3 was added in small portions during 0.5 h. The mixture turned dark green was heated to 75 ºC for 4 h, stirred for 10 h at room temperature and finally poured into a mixture of ice/water. The dark green precipitate was separated by centrifugation and washed several times with water. This green powder was then suspended in water and KOH was added under vigorous stirring until the solution was basic. The green insoluble residual powder was filtered and washed with water. The aqueous solution was acidified with dilute hydrochloric acid to precipitate the diacid *i.e.*, 2,2'-bipyridyl-4,4'-dicarboxylic acid which was filtered, washed with water, ethanol followed by ether and dried to give the pure diacid **2** as a white powder (5.8 g, 92.1 % yield and purity 95.7 %).

Synthesis of *cis*-$Ru^{II}L_2Cl_2·2H_2O$: It was obtained by refluxing under reduced light and N_2, 2.9 g (11 mmol) of $RuCl_3·3H_2O$ and 5.8 g (23.94 mmol) of 2,2'-bipyridyl-4,4'-dicarboxylic acid in 200 mL of DMF for 12 h[9]. After cooling, trace of $RuCl_3·2H_2O$ was filtered. Most of DMF solvent was evaporated under vacuum and *cis*-$Ru^{II}L_2Cl_2$ was precipitated with acetone. The crystals were filtered off and dried in vacuum at 55 ºC. In this way, 6.5 g of the brown product was obtained (6.5 g, 79.3 % yield and purity 96.0 %).

Synthesis of *cis*-$RuL_2(SCN)_2·2H_2O$[10]: 6.5 g (9.3 mmol) of *cis*-$Ru^{II}L_2Cl_2·2H_2O$ was dissolved in 30 mL DMF under reduced light and nitrogen atmosphere. To this solution was added aqueous NaOH (20 mL 0.1 M) in order to deprotonate the carboxy groups. Sodium thiocyanate (0.35 g) was separately dissolved in 2 mL of H_2O and subsequently added to the above solution. The reaction mixture was then heated to reflux for 6 h under nitrogen atmosphere, while magnetic stirring was maintained. After this time, the reaction mixture was allowed to cool and the solvent was removed on a rotary evaporator. The resulting solid was dissolved in H_2O and filtered through a sintered glass crucible. The pH of this filtrate was lowered to 2.5 by adding dilute $HClO_4$ and the filtrate was placed in a refrigerator overnight. After reaching room temperature, the microcrystalline solid was isolated by suction filtration, washed well with water/acetone-ether solution (1:10) followed by ether and dried under vacuum. 5.3 g (7.15 mmol) of purple solid was obtained (78.5 % yield and purity 97.4 %).

Preparation of the TiO_2 films: The TiO_2 film was obtained by sol-gel method[2]. The conducting glass substrate was covered on four edges with transparent adhesive tape to determine the film's thickness and size. TiO_2 sol was distributed with a glass rod sliding over the tape-covered edges. The obtained paste was spread over the conducting glass substrate. The film was then allowed to dry in air. After a few minutes, the tape was carefully removed and the film was heated to 450 ºC in air for 1 h. TiO_2 film was sensitized by *cis*-$RuL_2(SCN)_2·2H_2O$ in anhydrous ethanol (3 mmol/L) at 35 ºC for 3 h. Then the thin film was withdrawn from the solution and washed in anhydrous ethanol for testing. The sensitized TiO_2 film was charactered by IR and UV spectral studies.

Assemble device and determine output characteristics: The nanocrystalline photovoltaic cell (NPC) solar cell was assembled with dropping the electrolyte (a solution of 0.5 M potassium iodide and 0.05 M iodine in a mixture of *ca.* 80 % acetonitrile and 20 % glycol) into the space between

TiO_2 electrode and platinum mirror and connecting the external circuit. The dye-sensitized TiO_2 films were illuminated through the conductive glass support using a 500 W high pressure Xe lamp as the simulating sunlight. The short-circuit photocurrent and the open-circuit photovoltage were determined by photoelectricity parameter determination instrument.

RESULTS AND DISCUSSION

In the first step, 4-methylpyridine is both the solvent and reactant. A large amount of 4-methylpyridine did not participate in the reaction and can be reused in the coupling reaction again. The recovery ratio of palladium-catalyst is 90 % and it can be used repeatedly. This method largely decrease the cost of synthesizing *cis*-$RuL_2(SCN)_2{\cdot}2H_2O$. The catalysis mechanism and the probable side-reaction of the first step were studied using *ab initio* molecular orbital calculation (MO) method[12]. π Electron density of pyridine ring (Fig. 1) was caculated by MO method. The π electron density at *meta* position is 1.022, which increases 0.02 more than that at *ortho* position. It is well known that the nitrogen atom as a π electron acceptor in pyridine can decrease π electron density of its *ortho* position, whereas methyl group as a donating group can increase π electron density of its *ortho* and *meta* positions. Moreover, the presence of π electron donating group in a monosubstituted bipyridine increases the π electron density at the *ortho* position more than *meta* position. As a result, the π electron densitiy at C_2 is less than that at C_3. Since the main reaction of 2,2'-bipyridine series is mucleophilic substitution, it may expected that substitution reaction at 2 position in 4-methylpyridine should be more favored than at the 3. So, the main product is 4,4'-dimethyl-2,2'-bipyridine instead of 4,4'-dimethyl-3,3'-bipyridine or 4,4'-dimethyl-2,3'-bipyridine.

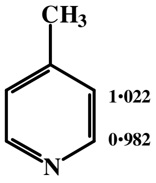

Fig. 1. Distribution of π-electron density of pyridine

MS-GC was used to analysis the structure of the product. It can be seen from Fig. 2 that there is a single sharp peak in the GC patterns, which indicated that there was mainly only one product. It is concluded from MS spectra that m/z = 184 is molecular ion peak of substitutive bipyridine, m/z = 169 is ion peak of the bibipyridine loss -CH_3; m/z = 92 is the ion peak after C-C between bipyridine breaking and m/z = 77 is the ion peak of the m/z = 92 which loss a -CH_3. So, it is concluded primarily that the product is 4,4'-dimethyl-2,2'-bipyridine.

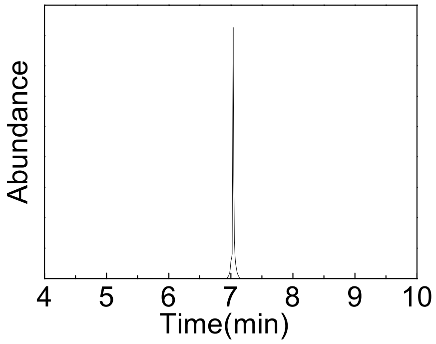

Fig. 2. GC result of the raw-product

Further studies on the structure of the product were based on ^{1}H NMR, IR and element analyse. m.p. 175-176 ºC[12]. ^{1}H NMR (DMSO): 8.52 (d, J = 4.9 Hz, 2H), 8.23 (s, 2H), 7.27 (d, J = 4.9 Hz, 2H), δ 2.41 (s, 6H, CH_3). IR (KBr, ν_{max}, cm^{-1}): 1604, 1563, 1461, 1428, 1372, 766 cm^{-1}. Anal. calcd for $C_{12}H_{12}N_2$: C 78.26, H 6.52, N 15.22; found C 78.26, H 6.89, N 14.87. MS (EI) m/z (rel. int.): m/z = 184, m/z = 169, m/z = 92, m/z = 77.

CrO_3 and H_2SO_4 were selected as oxidants because this reaction has a moderate condition, which can avoid 4,4'-dimethyl-2,2'-bipyridine to decompose at high temperature. In IR spectra, there is a strong absorption peak at 1717 cm^{-1}, which indicates this compound has some same carbonyl groups. Further structural characterization of 2,2'-bipyridine-4,4'-dicarboxylic acid (**2**) was carried out by ^{1}H NMR, ^{13}C NMR and IR: 1717, 2453, 604, 1563, 1461, 766 cm^{-1}. ^{1}H NMR (D_2O): δ 8.47 (d, 2H); 8.05 (s, 2H); 7.57 (d, 2H). ^{13}C NMR: 172.8, 155.4, 149.5, 146.0, 123.2, 121.1.

The compound *cis*-$Ru^{II}L_2Cl_2{\cdot}2H_2O$ (**3**) is obtained in good yield by heating the solution of 2,2'-bipyridine-4,4'-dicarboxlic acid and $RuCl_3{\cdot}3H_2O$. IR and ^{1}H NMR are consistent with the expected. The peak at the 3432 cm^{-1} gives the evident of existing water in compound *cis*-$Ru^{II}L_2Cl_2{\cdot}2H_2O$ (**3**). The spectrum exhibits peaks at 1604, 1563 and 1461 cm^{-1}, which is characteristic the pyridine rings. The peak at 1711 cm^{-1} is caused by carbonyl groups. Further structural characterization of compound **3** was carried out by ^{1}H NMR, which is exactly equal as a previous report. IR: 3432, 1711, 1630-1600, 1604, 1563, 1461, 767 cm^{-1}. ^{1}H NMR (D_2O + NaOH): δ 9.13 (d, 2H, H_6); 8.59 (s, 2H, H_3); 8.39 (s, 2H, $H_{3'}$); 7.84 (dd, 2H, H_5); 7.42 (d, 2H, $H_{6'}$); 7.04 (dd,-2H, $H_{5'}$).

The fourth step is a kind of exchange reaction. The reaction mechanism shows in **Scheme-I**. At first, undersaturated reaction intermediate is synthesized through decomposing the ligand, which usually is the rate-determining step. Then, reaction intermediate reacts with another ligand very quickly.

$$ML_n \rightleftharpoons ML_{n-1} + L$$

$$ML_{n-1} + L' \rightleftharpoons ML'L_{n-1}$$

Scheme-I

Structural characterization of *cis*-$RuL_2(SCN)_2 \cdot 2H_2O$ (**4**) was carried out by IR spectrum. The spectrum exhibits peaks at 2110 and 1990 cm^{-1}, which is characteristic the *cis*-configuration of two thiocyanate ligands. The N-coordination of the thiocyanate group is confirmed by the presence of the ν(C=S) resonance at 769 cm^{-1}. Furthermore, the peak at 3430 cm^{-1} gives the evident of existing water in *cis*-$RuL_2(SCN)_2 \cdot 2H_2O$ (**4**). Further characterization is shown in ^{13}C NMR and ^1H NMR spectra. The proton decoupled ^{13}C NMR of the *cis*-$Ru(dcbpy)_2(NCS)_2$ show 12 resonance peaks consisting of six sets due to two different ligands. Besides these 12 peaks, there is a single resonance peak at 131.850 ppm, which is assigned to the carbon of the N-coordinated NCS. ^1H NMR spectrum shows six peaks in the aromatic region corresponding to two different pyridine ring protons, which is exactly equal as previous report[11]. ^1H NMR (D_2O + NaOD) δ: 9.55 (d, 2H, H_6); 8.94 (s, 2H, H_3); 8.77 (s, 2H, $H_{3'}$); 8.22 (d, 2H, H_5); 7.82 (d, 2H, $H_{6'}$); 7.52 (d, 2H, $H_{5'}$). IR (KBr, ν_{max}, cm^{-1}): 1720, 770, 2110, 2140. ^{13}C NMR: 171.5, 171.1, 158.7, 157.5, 153.1, 152.1, 144.3, 143.6, 131.8, 125.6, 124.5, 122.1, 121.8.

Absorption properties of TiO_2 thin film before and after sensitizing: The IR spectra of samples were recorded using KBr pellet in the region 4000-400 cm^{-1} at room temperature. From Fig. 3 shows significant changes in relative band intensities and band position. There are more peaks of the sensitized TiO_2 film than that of the bare TiO_2 film at 1800-1200 cm^{-1}, probable following the dye adsorption on titanium oxide. Concerning the band around 1615 cm^{-1} of the *cis*-$RuL_2(SCN)_2$, it is important to note that a band having exactly the same structure exists in the pure TiO_2/KBr spectrum. This suggests that this band could be partially related to the presence of physics-adsorbed water and/or hydroxyl groups. Thus, the 20 cm^{-1} peak shift to higher frequencies of the C=O stretching mode could be explained by strong adsorption and binding of the dye to TiO_2. The shift probable arises from chemical adsorption of the dyes onto the oxide particles *via* ester-like binding between the carboxylic acid groups and the hydroxyl group on the TiO_2 particles.

UV-Visible absorption spectrums of the TiO_2 films before and after sensitizing are compared in Fig. 4. The most notable feature in the UV-Visible spectra is that the absorption in visible light region is significantly enhanced of TiO_2 film after sensitizing. The spectrum of the sensitized film exhibit one π-π* intra ligand transition in the UV region and two MLCT

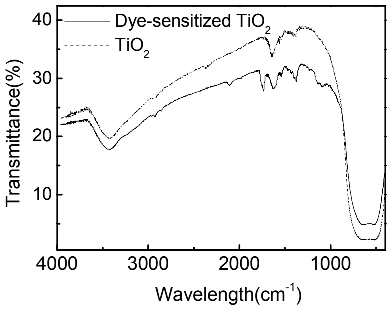

Fig. 3. IR spectrum of the TiO_2 thin film before and after sensitizing

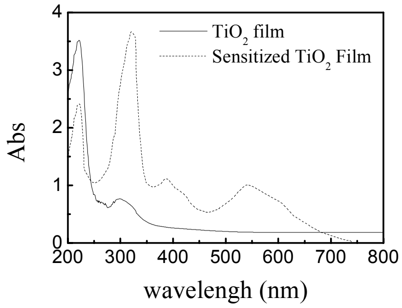

Fig. 4. UV-Visible spectrum of the TiO_2 thin film before and after sensitizing

(metal to ligand charge transfer transition) bands in the visible region. From discussion mentioned above, it is concluded that the dye has attached the surface of the TiO_2 particles, which is benefit to improve photoelectricity efficiency greatly.

Output characteristics: Fig. 5 shows photocurrent-voltage characteristics of the sell under white light illumination from 500W Xe lump (Table-1). The solar to electric conversion efficiency were determined using I-V curves. The result shows that the prepared *cis*-$RuL_2(SCN)_2 \cdot 2H_2O$ with this process can be used as sensitizer efficiently. The reason for this is that *cis*-$Ru(dcbpy)_2(NCS)_2$ belongs to organic metal complex compound which has a unique big π bond and transition element (Ru). This structure is benefit

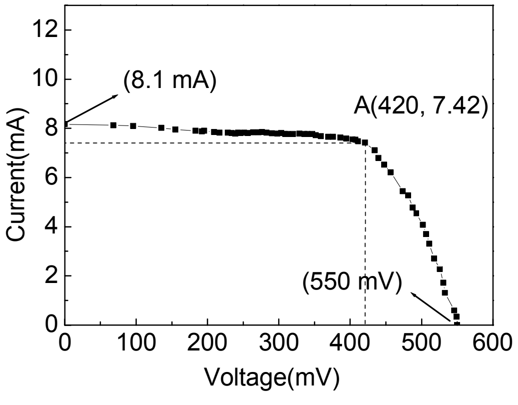

Fig. 5. Photocurrent-voltage characteristics of the sell

TABLE-1
SOLAR CELL PARAMETERS FOR THE RUTHENIUM COMPLEX

V_{OC} (mV)	I_{SC} (mA)	FF	η (%)
550	8.1	0.552	0.733

to deceasing energy of transferring electron and has strong absorption at 400-650 nm, which enlarge solar energy harvesting capacity. Ru(III/II) has a appropriate redox potential, which can supply driving force to transfer excitation electron to the conduction band of TiO_2. Moreover, *cis*-Ru(dcbpy)$_2$(NCS)$_2$ posses several carbonyl groups capable of chelating to the Ti(IV) sites on the titanium dioxide surface. The interaction between the carboxyl groups and the surface Ti ions is formed through C-O-Ti bonds, which can strengthen the couple between 3d orbit of conduction band of TiO_2 and π^* orbitals of *cis*-Ru(dcbpy)$_2$ (NCS)$_2$, which can transfer electron to conduction band of TiO_2 successfully. So, solar energy converts to the electric energy.

Conclusion

In conclusion, *cis*-RuL$_2$(SCN)$_2$·2H$_2$O was prepared as an a photosensitizer for the solar cell based on nanocrystalline TiO_2 semiconductor. There is excellent agreement between the experimental and predicted spectra of both the *cis* complex. In present studies, this efficient method has been developed for the preparation of *cis*-RuL$_2$(SCN)$_2$·2H$_2$O with high yields, moderate condition, simply purification, using recoverable and effective catalyst. Results show that highly pure *cis*-Ru(dcbpy)$_2$(NCS)$_2$ is prepared by this route and the total yield of the dye is 40.6 %. The recovered catalyst could be reused without any treatment. The dye is found to be good light to electricity converters on the TiO_2 surface through determining IR, UV-Visible spectrum and photocurrent-voltage characteristics. This approach provides a method to decrease the cost and be benefit to practical application of the solar energy cells.

ACKNOWLEDGEMENTS

The authors thank the National Natural Science Foundation of China (No. 50702018) and the Special Research project funded of Harbin Science, Technology Innovate Person with Ability (No. 2006RFQXS043) and Technology Innovate Fund of China Aerospace Science and Technology Corporation for the financial support for the financial support for this work.

REFERENCES

1. S. Anandan, J. Madhavan, P. Maruthamuthu, V. Raghukumar and V.T. Ramarkrishnan, *Sol. Energy Mater. Sol. Cells*, **81**, 419 (2004).
2. P. Falaras, *Sol. Energy Mater. Sol. Cells*, **53**, 163 (1998).
3. Y. Takahashi, H. Arakawa, H. Sugihara, K. Hara, A. Islam, R. Katoh, Y. Tachibana and M. Yanagida, *Inorg. Chim. Acta*, **310**, 169 (2000).
4. Z.Y. Wang, Z.G. Zha, J.H. Zhang and J.H. Wu, *Chin. Chem. Lett.*, **14**, 13 (2003).
5. X.C. Guo and R.J. Madix, *J. Catal.*, **155**, 336 (1995).

7. H.C. Foley and B.A. Raich, *Appl. Catal. A-Gen.*, **129**, 167 (1995).
8. N. Garelli and P. Vierling, *J. Org. Chem.*, **57**, 3046 (1992).
9. P. Liska, N. Vlachopoulos, K. Mohammad, C.P. Nazeerudiin and M. Gratzel, *J. Am. Chem. Soc.*, **110**, 3686 (1988).
10. M.K. Nazeeruddin, A. Kay, I. Rodicio, R. Humphry-Baker, E. Muller, P. Liska, N. Vlachopoulos and M. Gratzel, *J. Am. Chem. Soc.*, **115**, 6382 (1993).
11. J.E. Del Bene, *J. Am. Chem. Soc.*, **101**, 6184 (1979).
12. M.K. Nazeeruddin, S.M. Zakeeruddin, R. Humphry-Baker, S.I. Gorelsky, A.B.P. Lever and M. Gratzel, *Coord. Chem. Rev.*, **208**, 213 (2000).

(*Received*: 8 May 2007; *Accepted*: 1 February 2008) AJC-6272